HEPATOLOGY

HEPATOLOGY, VOL. 68, NO. 2, 2018

# Endothelial Notch Activation Reshapes the Angiocrine of Sinusoidal Endothelia to Aggravate Liver Fibrosis and Blunt Regeneration in Mice

Juan-Li Duan,[1*] Bai Ruan,[1,4*] Xian-Chun Yan,[2*] Liang Liang,[2] Ping Song,[1] Zi-Yan Yang,[2] Yuan Liu,[2] Ke-Feng Dou,[1] Hua Han,[1-3] and Lin Wang[1]

**Liver sinusoidal endothelial cells (LSECs) critically regulate liver homeostasis and diseases through angiocrine factors. Notch is critical in endothelial cells (ECs). In the current study, Notch signaling was activated by inducible EC-specific expression of the Notch intracellular domain (NIC). We found that endothelial Notch activation damaged liver homeostasis. Notch activation resulted in decreased fenestration and increased basement membrane, and a gene expression profile with decreased LSEC-associated genes and increased continuous EC-associated genes, suggesting LSEC dedifferentiation. Consistently, endothelial Notch activation enhanced hepatic fibrosis (HF) induced by $CCl_4$. Notch activation attenuated endothelial nitric oxide synthase (eNOS)/soluble guanylate cyclase (sGC) signaling, and activation of sGC by 3-(5′-hydroxymethyl-2′-furyl)-1-benzylindazole (YC-1) reversed the dedifferentiation phenotype. In addition, Notch activation subverted the hepatocyte-supporting angiocrine profile of LSECs by down-regulating critical hepatocyte mitogens, including Wnt2a, Wnt9b, and hepatocyte growth factor (HGF). This led to compromised hepatocyte proliferation under both quiescent and regenerating conditions. Whereas expression of Wnt2a and Wnt9b was dependent on eNOS-sGC signaling, HGF expression was not rescued by the sGC activator, suggesting heterogeneous mechanisms of LSECs to maintain hepatocyte homeostasis. *Conclusion:* Endothelial Notch activation results in LSEC dedifferentiation and accelerated liver fibrogenesis through eNOS-sGC signaling, and alters the angiocrine profile of LSECs to compromise hepatocyte proliferation and liver regeneration (LR). (HEPATOLOGY 2018; 68:677-690).**

Liver fibrosis (LF) is a common pathological process of end-stage liver diseases. Although LF is characterized by abnormal deposition of extracellular matrix, diminished hepatocyte regeneration is responsible for compromised liver function accounting for death.[1] Signals and mechanisms coordinating fibrogenesis and liver regeneration (LR) have not yet been fully clarified, hampering precision intervention of this pathology.

LSECs are specialized ECs lining liver sinusoids. These highly endocytic ECs exhibit a characteristic phenotype of nondiaphramed fenestrae and the lack of basal membrane, facilitating high-efficient material exchange between blood and the space of Disse (SD).[2-4] Normally, shear stress and vascular endothelial growth factor (VEGF) derived from hepatocytes and hepatic stellate cells (HSCs) maintain the LSEC phenotype, at least partly, through eNOS-sGC signaling.[5-8] During liver fibrogenesis, LSECs undergo

*Abbreviations: ALT, alanine aminotransferase; Angpt2, angiopoietin-2; AST, aspartate aminotransferase; BM, bone marrow; BM-SPCs, BM-derived LSEC progenitor cells; CM, conditional medium; Ctrl, control; Dll, delta-like ligand; ECs, endothelial cells; ELISA, enzyme-linked immunosorbent assay; eNOS, endothelial nitric oxide synthase; FITC, fluorescein isothiocyanate; FITC-FSA, FITC/formaldehyde-treated serum albumin; GSI, γ-secretase inhibitor; GUCY, guanylate cyclase; H&E, hematoxylin and eosin; Hes, hairy and enhancer of split; Hey1, hairy/enhancer-of-split related with YRPW motif protein 1; HGF, hepatocyte growth factor; IF, immunofluorescence; IHC, immunohistochemistry; LF, liver fibrosis; LR, liver regeneration; LSECs, liver sinusoidal endothelial cells; NIC, Notch intracellular domain; PDGFβ, platelet-derived growth factor beta; PHx, partial hepatectomy; RBP-J, recombination signal binding protein Jκ; RNA-seq, RNA-sequencing; SD, space of Disse; SEM, scanning electron microscopy; sGC, soluble guanylate cyclase; α-SMA, alpha-smooth muscle actin; TBIL, total bilirubin; TEM, transmission electron microscopy; TGF, transforming growth factor; TIMP-1, tissue inhibitor of metallopeptidase-1; TUNEL, terminal deoxynucleoitidyl transferase-mediated dUTP nick end labeling; VEGF, vascular endothelial growth factor; VEGFR, VEGF receptor; YC-1, 3-(5′-hydroxymethyl-2′-furyl)-1-benzylindazole.*

*Received September 13, 2017; accepted February 2, 2018.*

*Additional Supporting Information may be found at onlinelibrary.wiley.com/doi/10.1002/hep.29834/suppinfo.*

dedifferentiation called capillarization.[9-12] Dedifferentiated LSECs lose their fenestrae and express ECM to develop a basement membrane, leading to HSC activation and hepatocyte damage. LSEC dedifferentiation has been recognized as an initial pathological marker and is essential for LF, because blocking LSEC dedifferentiation with a sGC activator abrogates fibrogenesis in rodent models.[12,13]

In addition, LSECs also function as a niche to maintain hepatocyte homeostasis by angiocrine factors.[14-17] Gata4-dependent LSECs are required for liver development and hepatocyte proliferation.[4] LSECs secrete Wnt ligands and HGF to support replenishment and functional zonation of hepatocytes under steady state.[18-21] LSECs also contribute to LR.[14-17,22-24] In mice, partial hepatoctemy (PHx)-induced LR is accompanied by downregulation of angiopoietin-2 (Angpt2) and transforming growth factor (TGF)-$\beta$1, and increased secretion of Wnt2a and HGF through the VEGF receptor (VEGFR) 2/inhibitor of differentiation-1 (Id1) pathway in LSECs, leading to enhanced hepatocyte proliferation on day 2.[19,25] VEGFR2-Id1 signaling and re-expressed Angpt2 also promote LSEC-mediated angiogenesis on day 4 post-PHx to re-establish hepatic circulation.[19,25] Moreover, stromal-derived factor-1 and its receptors, C-X-C chemokine receptor (CXCR)4 and CXCR7, control a balance between LR and fibrosis.[26] However, a relationship between LSEC dedifferentiation and angiocrine and the underlying mechanisms have not been completely elucidated.

Notch signaling is evolutionarily highly conserved and regulates vasculogenesis, angiogenesis, and vascular remodeling.[27,28] Triggering Notch receptors activates proteolytic cleavages catalyzed by $\gamma$-secretase, liberating the Notch intracellular domain (NIC). NIC enters nucleus to activate transcription of downstream molecules, such as the hairy and enhancer of split (Hes) family members, through the transcription factor, recombination signal-binding protein J$\kappa$ (RBP-J).[27] In quiescence, Notch2 is highly expressed by LSECs, whereas Jagged1, delta-like ligand (Dll)1, and Dll4 are expressed at low level.[3] Previous studies have shown that deficiencies in Notch1 or RBP-J in adult mice disrupted sinusoidal and hepatocyte homeostasis.[29-31] However, the overall consequence of Notch activation in LSECs has not been assessed. In this study, we report that activation of Notch

*Supported by grants from: MOST (2016YFA0102100 [The National Key Research and Development Program of China: Stem Cell and Translational Research], 2015CB553702), and NSFC (91339115 [the major research program "Regulation mechanisms of blood vessel homeostasis and remodeling"], 81422009, 81401940, 81370512, 81770560, 31730041, 31671523, 31370769, 81200707, and 31301194).*

**These authors contributed equally to this study.*



*View this article online at wileyonlinelibrary.com.*

*DOI 10.1002/hep.29834*

*Potential conflict of interest: Nothing to report.*

## ARTICLE INFORMATION:

**From the [1]Department of Hepatobiliary Surgery, Xi-Jing Hospital, Fourth Military Medical University, Xi'an, China; [2]State Key Laboratory of Cancer Biology, Department of Medical Genetics and Developmental Biology, Fourth Military Medical University, Xi'an, China; [3]Department of Biochemistry and Molecular Biology, Fourth Military Medical University, Xi'an, China; and [4]Department of Clinical Aerospace Medicine, School of Aerospace Medicine, Fourth Military Medical University, Xi'an, China.**

## ADDRESS CORRESPONDENCE AND REPRINT REQUESTS TO:

**Lin Wang, M.D., Ph.D.**
**Department of Hepatobiliary Surgery, Xi-Jing Hospital, Fourth Military Medical University**
**Chang-Le Xi Street #169,**
**Xi'an 710032, China**
**E-mail: fierywang@163.com**
**Tel: +(86)-29-83246270; or**
**Hua Han, Ph.D.**
**Department of Biochemistry and Molecular Biology, Fourth Military Medical University**
**Chang-Le Xi Street #169, Xi'an 710032, China**
**E-mail: huahan@fmmu.edu.cn**
**Tel: +(86)-29-83246270; or**
**Ke-Feng Dou, M.D., Ph.D.**
**Department of Hepatobiliary Surgery, Xi-Jing Hospital, Fourth Military Medical University**
**Chang-Le Xi Street #169,**
**Xi'an 710032, China**
**E-mail: doukef@fmmu.edu.cn**
**Tel: +(86)-29-83246270**

signaling in ECs led to LSEC dedifferentiation and enhanced LF, and altered LSEC angiocrine spectrum that attenuated LR.

# Materials and Methods

## MICE

Mice were maintained in a specific pathogen-free facility on the C57BL/6J background. ROSA-STOP$^{floxed}$-NIC mice (murine Notch1 NIC [1749-2293] followed by IRES-GFP in the ROSA26 locus; Jackson Laboratory, Bar Harbor, ME) were crossed with the CDH5-CreERT mice (kindly provided by R.H. Adams).[32] Littermates were genotyped by PCR to obtain CDH5-CreERT (control; Ctrl) and CDH5-CreERT-NIC (NIC$^{eCA}$) mice. Male mice (6 weeks old) were injected intraperitoneally with tamoxifen (100 mg/kg; Sigma-Aldrich, St. Louis, MO) totally for seven injections (Fig. 1A).[33] Mice were kept for 1 more week to minimize potential influence from tamoxifen before further analyses. In some cases, from the third injection of tamoxifen, mice were injected simultaneously with 3-(5′-hydroxymethyl-2′-furyl)-1-benzylindazole (YC-1; 5 mg/kg; Sigma-Aldrich) for 7 times in total (Fig. 1A).[13] PHx was performed as described.[29] To induce LF, mice were injected intraperitoneally with 0.6 mL/kg of $CCl_4$ (Sigma-Aldrich) twice a week for 6 weeks, with olive oil as a control. To measure portal pressure, mice were anesthetized and the portal vein was punctured with a 25-G needle connected to a sensor and the MedLab-U/4C501 Bioinformation Collecting and Processing System (Zhong Shi Di Chuang Sci&Technol Dev Co., Ltd, Beijing, China). Stable pressure of portal vein was recorded and processed automatically.

All animal experiments were reviewed and approved by the Animal Experiment Administration Committee of the Fourth Military Medical University (Xi'an, China) to ensure ethnical and humane treatment of animals. The study followed the guideline outlined in the National Institutes of Health Guide for the Care and Use of Laboratory Animals prepared by the National

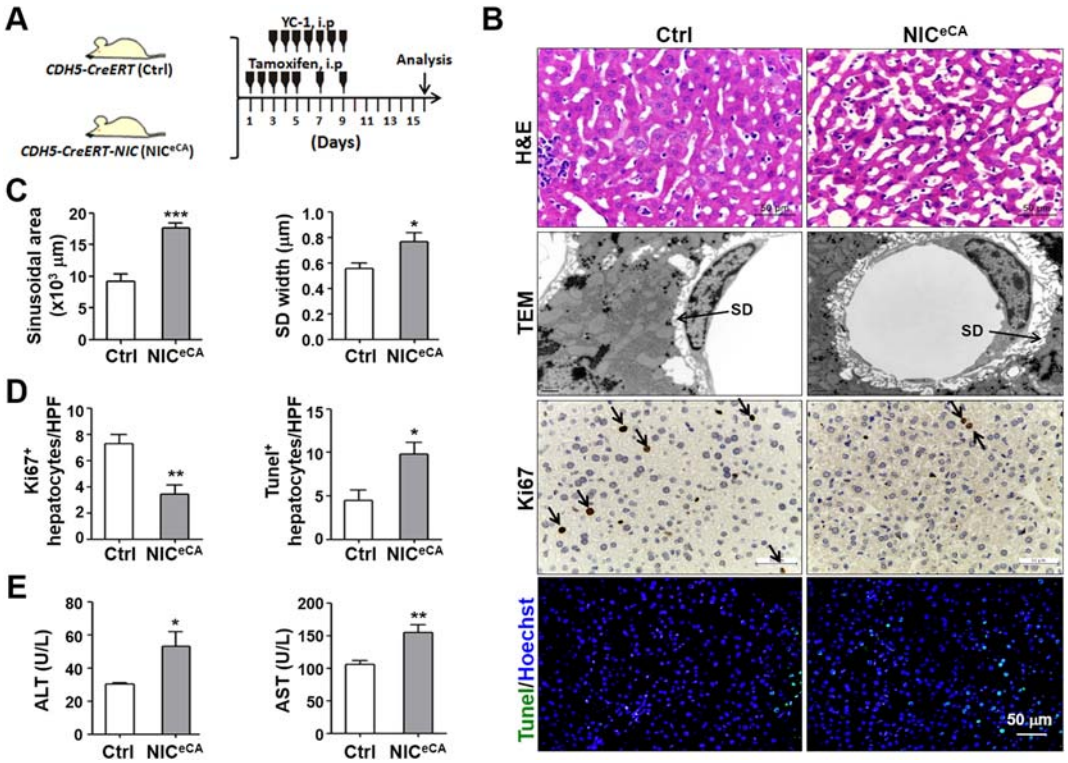


**FIG. 1.** Endothelial Notch activation disrupted liver homeostasis. (A) Genotypes of mouse models and schedules for tamoxifen and YC-1 injection. (B) Liver sections from NIC$^{eCA}$ and control mice were analyzed with H&E staining, TEM, anti-Ki67 IHC, and TUNEL. Ki67$^+$ hepatocytes are indicated with arrows. (C) Sinusoid areas and width of SD. (D) The numbers of Ki67$^+$ and TUNEL$^+$ hepatocytes were compared between NIC$^{eCA}$ and control mice. (E) Serum level of ALT and AST in NIC$^{eCA}$ and control mice was determined. Bars = means ± SD, n = 6; $^*P < 0.05$; $^{**}P < 0.01$; $^{***}P < 0.001$.

Academy of Science and published by the National Institute of Health (publications 86-23, revised 1985).

Human liver cirrhosis (LC) and hepatic hemangioma samples were obtained from patients in the Department of Hepatobiliary Surgery, Xi-Jing Hospital. All subjects involved were given informed consent for use of their tissues for research purposes. The use of human tissues for this study was approved by the Ethics Committee, Xi-Jing Hospital.

## HISTOLOGY

Liver samples were fixed in 10% buffered formalin or in 4% paraformaldehyde (PFA). Formalin-fixed samples were paraffin-embedded, sectioned, and stained with hematoxylin and eosin (H&E) routinely. PFA-fixed samples were embedded with optimum cutting temperature compound and sectioned at 8-$\mu$m thickness. For immunohistochemistry (IHC), sections were incubated with primary antibodies at 4°C overnight, washed, and incubated with horseradish peroxidase–conjugated secondary antibodies for 2 hours at room temperature. Sections were then developed using a 3,3′-diaminobenzidine substrate kit (Zhongshan Jinqiao Biotech, Beijing, China). Immunofluorescence (IF) was performed using fluorescent antibodies and counterstained with Hoechst 33258 (Sigma-Aldrich). Antibodies are listed in Supporting Table S1. Fluorescein isothiocyanate (FITC) or DyLight 594–conjugated Isolectin B4 (Vector Laboratories, Burlingame, CA) was used in staining with the same protocol. Apoptotic cells were stained with a terminal deoxynucleoitidyl transferase-mediated dUTP nick end labeling (TUNEL) kit (Promega, Madison, WI). Digital images were taken under a fluorescence microscope (BX51; Olympus, Tokyo, Japan) or laser-scanning confocal fluorescence microscope (FV-1000; Olympus). Transmission electron microscopy (TEM) and scanning electron microscopy (SEM) were carried out as described.[29]

## CELL ISOLATION AND CULTURE

Hepatocytes and liver nonparenchymal cells were isolated as described, with modifications.[29] Briefly, mice were anesthetized and perfused with Hank's buffer without $Ca^{2+}$ from the portal vein, followed by Hank's buffer with $Ca^{2+}$ and $Mg^{2+}$ containing 0.2 mg/mL of collagenase IV (Sigma-Aldrich). The liver was removed and finely minced with a tissue homogenizer in perfusion buffer containing 0.2 mg/mL of collagenase IV and 10 $\mu$g/mL of DNase I (Roche, Basel, Switzerland). Single-cell suspension was generated by passing through a 70-$\mu$m cell mesh and resuspended in Hank's buffer. Hepatocytes were pelleted by low-speed centrifugation at 50*g* for 3 minutes and resuspended in Hank's buffer, followed by three washes with Hank's buffer to remove cell debris. Supernatants were further centrifuged at 400*g* for 8 minutes to recover LSECs. Pelleted cells were resuspended in 4 mL of 17.6% iodixanol (Axis-Shield Diagnostics Ltd., Tarrytown, NY) and 4 mL of 8.2% iodixanol and 2 mL of Dulbeccoo's modified Eagle's medium (DMEM; Invitrogen, Carlsbad, CA) were orderly loaded on the top of the cell suspension. The cell suspension was then centrifuged at 1,400*g* for 20 minutes in a swing-out rotor without brake. LSECs were recovered from the interface between the 8.2% and 17.6% iodixanol solutions, mixed with an equal volume of DMEM and centrifuged at 400*g* for 8 minutes. Cells were resuspended and incubated with anti-CD146 magnetic beads (Miltenyi Biotec, Bergisch Gladbach, Germany) for 15 minutes at 4°C in dark. Cells were then washed with the washing buffer (phosphate-buffered saline [PBS] containing 2 mM of ethylenedimainetetraacetic acid and 0.5% bovine calf serum [bovine serum albumin]; pH 7.2) and resuspended in 1 mL of the washing buffer. The cell suspension was then applied onto the magnetic column of a MACS separator, and washed with 500 $\mu$L of the washing buffer for three times. Finally 1 mL of the washing buffer was loaded on the MACS column, and LSECs were immediately flushed out.

Hepatocytes were cultured in collagen I–coated plates with hepatocyte medium (ScienCell, San Diego, CA), supplemented with 5% fetal bovine serum (GIBCO, Rockville, MD), 1% hepatocyte growth supplement, 2 mM of L-glutamine, 100 $\mu$g/mL of streptomycin, and 100 U/mL of penicillin. HGF (50 ng/mL; Sigma-Aldrich) or Wnt2a-containing conditional medium (CM; collected from *HEK293T* cells transfected with an Wnt2a-expressing vector) was added and incubated for 20 hours. Hepatocyte proliferation was determined with anti-Ki67 IF. LSECs were cultured in collagen I–coated 24-well plates with EC medium supplemented with EC growth solution (ScienCell). GSI IX (Sigma-Aldrich), mD1R,[34] or YC-1 was added at concentrations of 75 $\mu$M, 5 $\mu$g/mL, and 30 $\mu$M, respectively.

## ENDOCYTOSIS

Endocytosis of LSECs *in vivo* was assayed using FITC/formaldehyde-treated serum albumin (FITC-FSA), according to published protocols.[35]

## GENE EXPRESSION PROFILING

RNA was extracted, sequenced, and analyzed by custom service provided by RiboBio (Guangzhou, China) using an Illumina HiSeq3000 (Illumina, San Diego, CA). Briefly, total RNA was extracted from LSECs isolated from $NIC^{eCA}$ or control mice using TRIzol (Invitrogen), according to the manufacturer's protocol. RNA integrity was evaluated using the Agilent 2200 TapeStation (Agilent Technologies, Santa Clara, CA), and each sample had the RINe above 7.0. mRNA was isolated and fragmented to approximately 200 base pairs (bp) in length and subjected to complementary DNA (cDNA) synthesis followed by adaptor ligation and enrichment with a low-cycle PCR using the TruSeq RNA LT/HT Sample Prep Kit (Illumina). Purified library products were evaluated using the Agilent 2200 TapeStation and Qubit2.0 (Life Technologies, Carlsbad, CA) and then diluted to 10 pM for cluster generation *in situ* on the HiSeq3000 pair-end flow cell followed by sequencing (2 × 150 bp) on HiSeq3000. Original data were deposited in the Gene Expression Omnibus database (accession no.: GSE102419). Bioinformatic analysis was performed using the OmicShare tools at www.omicshare.com/tools.

## RT-PCR

Total RNA was prepared by using TRIzol and reverse-transcribed into cDNA with the PrimeScrip RT reagent kit (TaKaRa Biotechnology, Dalian, China). Quantitative real-time PCR (qPCR) was performed using the SYBR premix ExTaqII (TaKaRa Biotechnology) and Applied Biosystems 7500 Real-time PCR system (Applied Biosystems, Foster City, CA), with $\beta$-actin as a reference control. Primers are listed in Supporting Table S2.

## WESTERN BLOTTING

Total protein was extracted with the radioimmunoprecipitation assay lysis buffer, containing 10 mM of phenylmethanesulfonyl fluoride, and quantified with a bicinchoninic acid assay protein assay kit (Thermo Fisher Scientific, Rockford, IL). Samples were separated with sodium dodecyl sulfate/polyacrylamide gel electrophoresis and transferred onto polyvinylidene fluoride membranes. Blottings were incubated with primary antibodies followed by HRP-conjugated secondary antibodies (Supporting Table S1) and developed with enhanced chemiluminescence (Clinx Science Instruments, Shanghai, China).

## ENZYME-LINKED IMMUNOSORBENT ASSAY AND BIOCHEMISTRY

HGF in culture supernatants was analyzed with an enzyme-linked immunosorbent assay (ELISA) kit (eBioscience/Thermo Fisher Scientific). Serum levels of alanine aminotransferase (ALT) and aspartate aminotransferase (AST) were determined with a Chemistry Analyzer (AU400; Olympus). Hydroxyproline was determined with a kit (Jiancheng Bioengineering Institute, Nanjing, China).

## STATISTICAL ANALYSIS

Statistical analysis was performed with the SPSS (version 12.0; SPSS, Inc., Chicago, IL) program. Comparisons between groups were undertaken using the unpaired Student *t* test. Results are expressed as means ± SD. $P < 0.05$ was considered statistically significant.

# Results

## ENDOTHELIAL Notch ACTIVATION DAMAGED LIVER HOMEOSTASIS

In tamoxifen-induced $NIC^{eCA}$ mice (Fig. 1A),[32] expression of Hes1 and hairy/enhancer-of-split related with YRPW motif protein 1 (Hey1), two target genes of canonical Notch signaling, was up-regulated significantly in LSECs isolated from $NIC^{eCA}$ mice, suggesting Notch activation (Supporting Fig. S1C). No gross abnormality was noticed systemically or in liver of $NIC^{eCA}$ mice (Supporting Fig. S1D,E). However, in quiescent $NIC^{eCA}$ mice, the area of liver sinusoids increased significantly (Fig. 1B,C) with widened SD as shown by TEM (Fig. 1B,C). $Ki67^{+}$ hepatocytes decreased whereas $TUNEL^{+}$ hepatocytes increased as compared to the control (Fig. 1B,D), suggesting reduced proliferation and increased apoptosis. The level of serum ALT and AST increased (Fig. 1E). These data suggested that EC-specific Notch activation impaired liver homeostasis under steady state in mice.

## ENDOTHELIAL Notch ACTIVATION LED TO LSEC DEDIFFERENTIATION

Density of LSECs decreased, as shown by anti-Lyve-1 IF and isolectin staining (Fig. 2A), accompanied by increased apoptosis as detected by TUNEL (Fig. 2A). Endocytic capacity of LSECs, as shown by uptake of FITC-FSA, decreased remarkably in $NIC^{eCA}$ mice, suggesting LSEC dysfunction (Fig. 2B; Supporting Fig. S2).

Gene expression profiling showed that LSECs from $NIC^{eCA}$ mice expressed decreased LSEC-associated genes, but increased continuous EC-associated genes (Fig. 2C).[4] qRT-PCR confirmed that expression of capillary EC markers laminin, CD31, and endothelin-1 (ET-1) was up-regulated in LSECs with activated Notch signaling (Fig. 2D). Ultrastructure under SEM indicated that the number of fenestrae in LSECs decreased significantly in $NIC^{eCA}$ mice (Fig. 2E). IF indicated that Notch activation led to increased expression of laminin by LSECs (Fig. 2E). In summary, these data demonstrated that Notch activation resulted in LSEC dedifferentiation.

## ENDOTHELIAL Notch ACTIVATION AGGRAVATED $CCl_4$-INDUCED LF

Induction of LF in $NIC^{eCA}$ and control mice $CCl_4$ showed that $NIC^{eCA}$ mice manifested significantly aggravated fibrogenesis, as evidenced by increased ECM deposition detected by Sirius Red staining (Fig. 3A), and elevated tissue hydroxyproline level (Fig. 3A). IF showed increased Desmin (Fig. 3B) and alpha-smooth muscle actin (α-SMA; Fig. 3B) staining, suggesting enhanced HSC activation after endothelial Notch activation. In fibrotic $NIC^{eCA}$ mice, less liver sinusoid fenestrae (Fig. 3C) and a higher level of

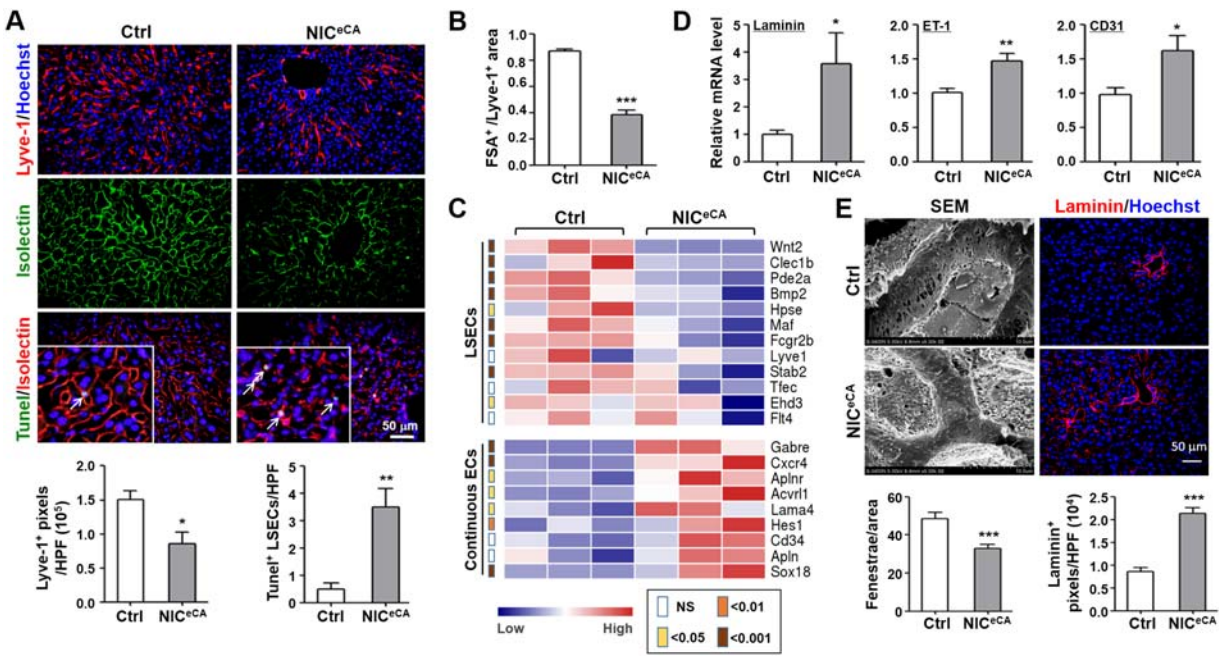


**FIG. 2.** Endothelial Notch activation led to LSEC dedifferentiation. (A) Liver sections from $NIC^{eCA}$ and control mice were stained with anti-Lyve-1, isolectin-FITC, and TUNEL. Lyve-$1^+$ pixels and $TUNEL^+$ cells in $lectin^+$ LSECs were quantitatively compared. (B) $NIC^{eCA}$ and control mice were injected with FITC-FSA through the tail vein. Mice were sacrificed 1 hour later, and liver sections were stained with anti-Lyve-1 IF (Supporting Fig. S2). FITC-FSA pixels were calibrated with Lyve-1pixels and compared. (C) LSECs were isolated from $NIC^{eCA}$ and control mice. Gene expression profiles were analyzed with RNA-seq, and expression of LSEC-associated genes and continuous EC-associated genes were compared with a heatmap. The *P* value of each comparison was indicated with colors. (D) Expression of laminin, ET-1, and CD31 was determined with qRT-PCR. (E) Liver sections from $NIC^{eCA}$ and control mice were analyzed using SEM and antilaminin IF. LSEC fenestrae and the relative level (pixels) of laminin were quantitatively compared. Bars = means ± SD, n = 6; $^*P < 0.05$; $^{**}P < 0.01$; $^{***}P < 0.001$.

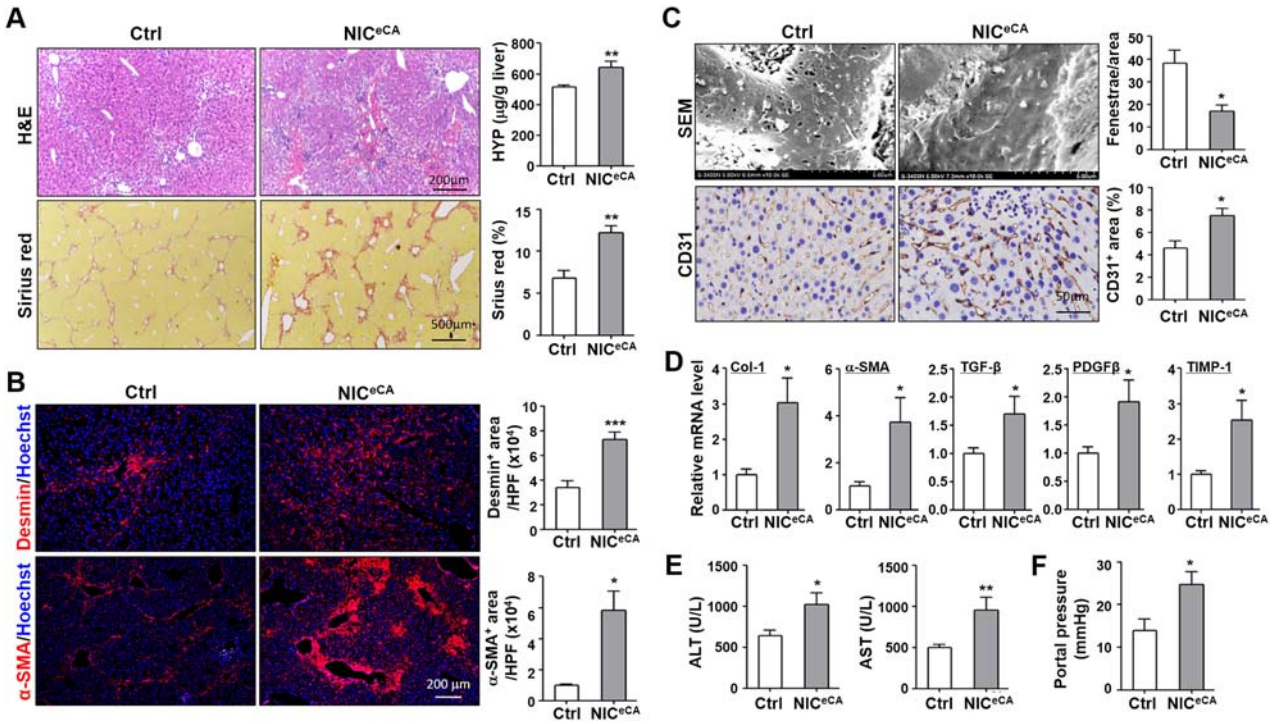


**FIG. 3.** Endothelial Notch activation aggravated $CCl_4$-induced LF. (A) Liver sections from $CCl_4$-induced fibrotic liver were stained with H&E and Sirius Red. Sirius Red$^+$ areas were quantified and compared. Hydroxyproline level in liver extracts was measured. (B) Liver sections were stained with anti-Desmin and anti-α-SMA IF. Desmin$^+$ and α-SMA$^+$ areas were compared. (C) Liver sections from $CCl_4$-induced fibrotic liver were analyzed using SEM and anti-CD31 IHC. LSEC fenestrae and CD31$^+$ areas were quantitatively compared. (D) mRNA level of collagen-1, α-SMA, TGF-*β*, PDGF*β*, and TIMP-1 in fibrotic liver was quantified by qRT-PCR. (E) Serum level of ALT and AST in fibrotic mice was determined. (F) Portal pressure of fibrotic mice was determined. Bars = means ± SD, n = 6; $^*P < 0.05$; $^{**}P < 0.01$; $^{***}P < 0.001$.

capillary marker CD31 (Fig. 3C) were observed. Consistent with enhanced fibrogenesis, elevated expression of fibrosis-related genes, including collagen-1, α-SMA, TGF-*β*, platelet-derived growth factor beta (PDGF*β*), and tissue inhibitor of metallopeptidase-1 (TIMP-1), in LSECs was detected (Fig. 3D). We also observed higher serum ALT and AST (Fig. 3E), and higher portal pressure (Fig. 3F), in NIC$^{eCA}$ mice, consistent with increased hepatocyte injury and portal resistance. Moreover, to access the clinical relevance of our findings, we collected liver biopsies from patients with or without cirrhosis, and performed IHC to detect nuclear Notch1 intracellular domain (N1IC) in LSECs. The result showed that in the liver of patients with cirrhosis, the number of LSECs with nuclear N1IC increased significantly as compared to that of patients without cirrhosis, suggesting a role of Notch activation in LSECs during LC (Supporting Fig. S3A,B). These data collectively indicated that endothelial Notch activation resulted in aggravated LF associated with LSEC dedifferentiation.

## Notch ACTIVATION-INDUCED LSEC CAPILLARIZATION WAS eNOS-sGC DEPENDENT

Further analysis of RNA-sequencing (RNA-seq) data suggested that a set of genes in eNOS-sGC signaling, which participates in maintaining LSEC phenotypes, were changed upon Notch activation (Fig. 4A).[13] Then, we examined expression of molecules involved in this pathway. The result showed that mRNA level of VEGFR2, VEGFR3, and eNOS decreased, whereas expression of Angpt2 increased significantly in LSECs isolated from NIC$^{eCA}$ mice (Fig. 4B). Western blotting confirmed that in LSECs from NIC$^{eCA}$ mice, Hes1 was up-regulated whereas VEGFR2, eNOS, and phosphorylated eNOS decreased (Fig. 4C,D). Blockade of Notch signaling by γ-secretase inhibitor (GSI) *in vitro* showed decreased expression of eNOS and VEGFR2, and increased Angpt2, whereas VEGFR3 mRNA level remained unchanged (Fig. 4E). Treatment of normal

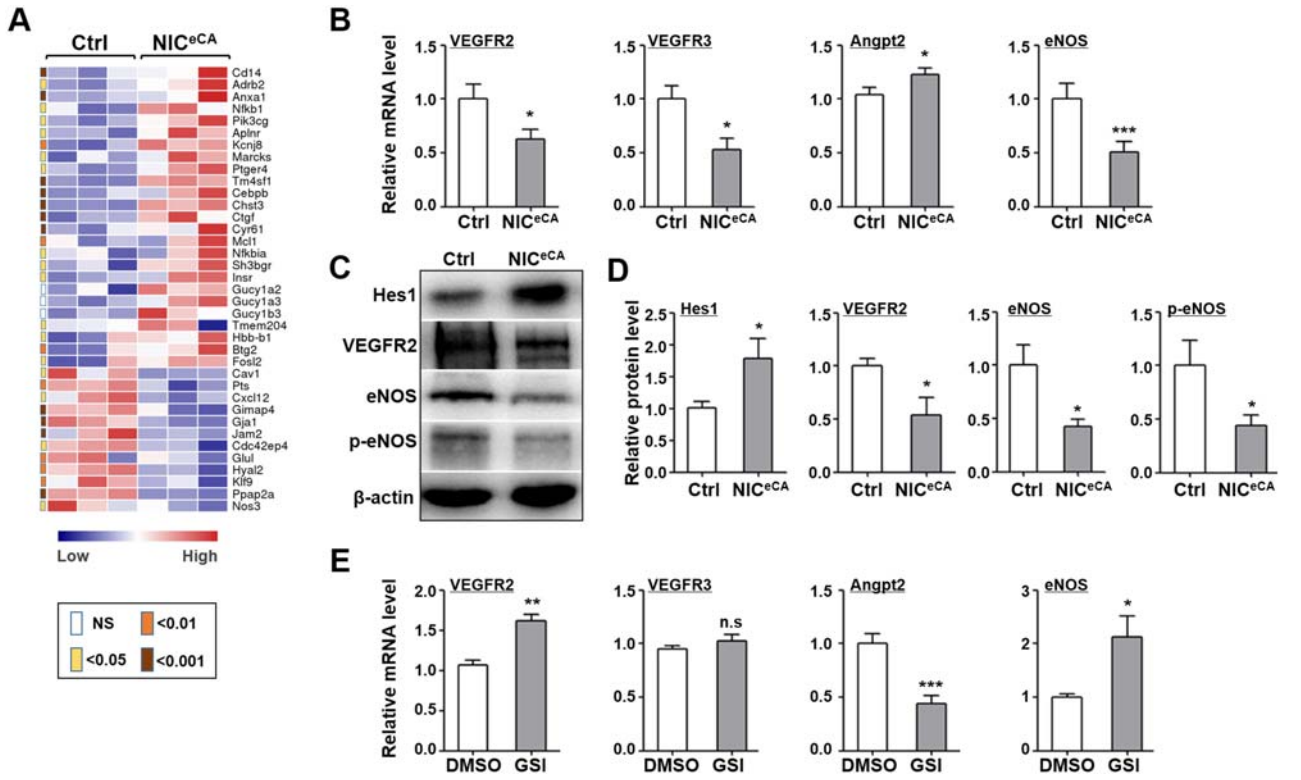


**FIG. 4.** Endothelial Notch activation down-regulated VEGFR2 and eNOS. (A) Heatmap comparison of eNOS-sGC signal-related genes (http://software.broadinstitute.org/gsea/msigdb/search.jsp) with RNA-seq data derived from NIC$^{eCA}$ and control LSECs (Fig. 2C). (B) LSECs were magnetically isolated from NIC$^{eCA}$ and control mice. Expression of VEGFR2, VEGFR3, Angpt2, and eNOS was determined by qRT-PCR, with $\beta$-actin as an internal control. (C,D) Cell extracts were prepared from LSECs in (B). Protein levels of Hes1, VEGFR2, eNOS, and p-eNOS were determined by western blotting (C) and quantitatively compared (D), with $\beta$-actin as a reference control. (E) LSECs from normal mice were treated with GSI or DMSO *in vitro*, and expression of VEGFR2, VEGFR3, Angpt2, and eNOS was determined using qRT-PCR, with $\beta$-actin as an internal control. Bars = means ± SD, n = 6; $^{*}P < 0.05$; $^{**}P < 0.01$; $^{***}P < 0.001$. Abbreviations: DMSO, dimethyl sulfoxide; n.s, not significant; p-eNOS, phosphorylated eNOS.

LSECs with a Notch ligand protein, mD1R,[34] reduced expression of VEGFR2 and eNOS, and up-regulated Angpt2 (Supporting Fig. S4A). Expression of VEGFR1 and sGC components, including guanylate cyclase (GUCY)1A2, GUYC1A3, and GUYC1B3, was not influenced significantly by Notch activation and blockade (Supporting S4B,C). These data suggested that Notch activation might result in LSEC dedifferentiation through repressing expression and/or activity of eNOS-sGC.

NIC$^{eCA}$ and control mice were injected with YC-1, an sGC activator (Fig. 1A).[13] LSEC dedifferentiation induced by Notch activation, characterized by decreased fenestrae and increased laminin expression, was abrogated by YC-1, as shown by SEM and immunofluorescence staining (Fig. 5A-C). Laminin was colocalized with Lyve-1, confirming that it was likely derived from LSECs (Fig. 5A). The reduced number of Lyve-1$^{+}$ LSECs induced by Notch activation was also rescued by YC-1 (Fig. 5D). qRT-PCR confirmed the down-regulation of laminin in LSECs from NIC$^{eCA}$ mice injected with YC-1 (Fig. 5E). These results suggested that Notch activation led to a down-regulated eNOS-sGC pathway, which was responsible for LSEC dedifferentiation.

## ENDOTHELIAL Notch ACTIVATION IMPEDED LR POST-PHx

Normal mice were subjected to PHx, and LSECs were isolated on days 1, 2, 4, 6, and 8 after the operation or from the sham group. qRT-PCR showed that the mRNA levels of Dll4, Notch1, Hes1, and Hey1 were markedly reduced on day 2 post-PHx, but recovered eventually and reached a normal level on day 8 (Fig. 6A). To examine whether endothelial Notch activation influences LR, we performed PHx in NIC$^{eCA}$ and control mice. The result showed that NIC$^{eCA}$ mice exhibited significantly retarded LR post-

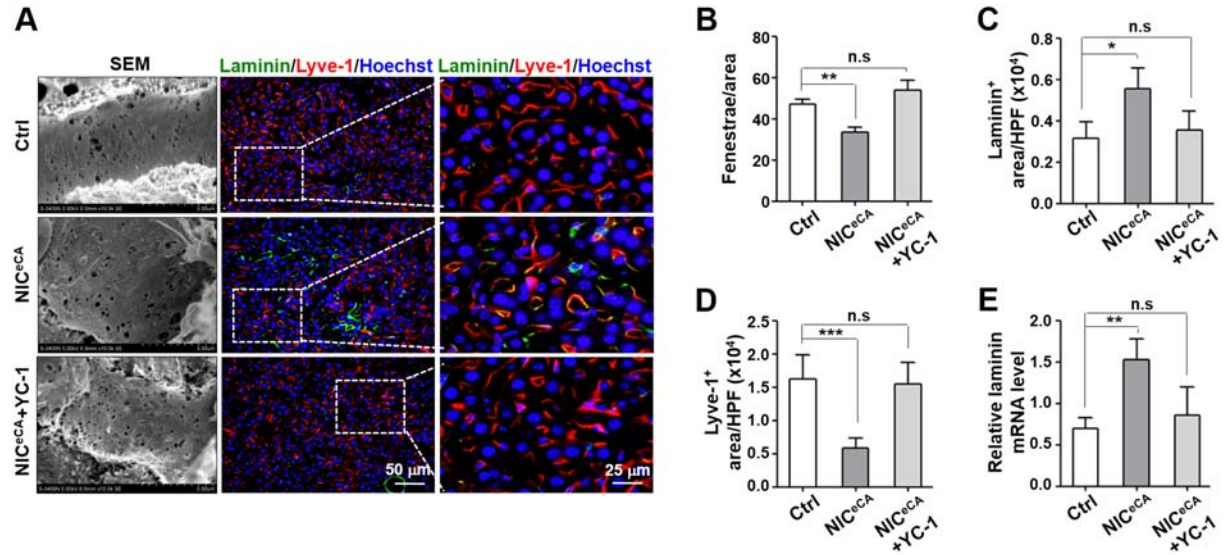


**FIG. 5.** YC-1 reversed LSEC dedifferentiation caused by endothelial Notch activation. (A) NIC$^{eCA}$ and control mice were injected intraperitoneally with YC-1 (Fig. 1A). Liver sections were analyzed by SEM, antilaminin, and anti-Lyve-1 IF. (B-D) LSEC fenestrae (B), laminin$^{+}$ pixels (C), and Lyve-1$^{+}$ pixels (D) were quantitatively compared. (E) LSECs were isolated from mice in (A), and expression of laminin was determined using qRT-PCR, with $\beta$-actin as an internal control. Bars = means ± SD, n = 6; $^{*}P < 0.05$; $^{**}P < 0.01$; $^{***}P < 0.001$. Abbreviation: n.s, not significant.

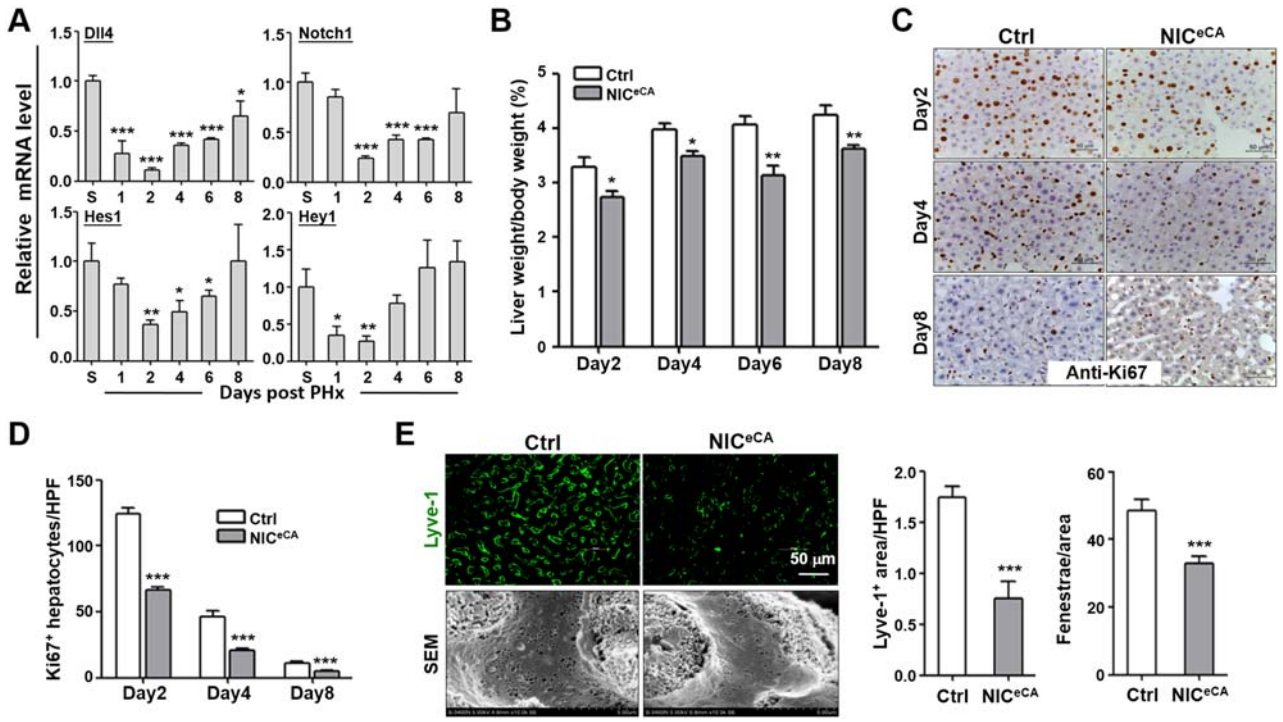


**FIG. 6.** Endothelial Notch activation resulted in compromised hepatocyte proliferation during LR. (A) Normal mice were subjected to PHx. LSECs were isolated on indicated days (S, sham-operated), and expression of Dll4, Notch1, Hes1, and Hey1 was determined using qRT-PCR. (B) NIC$^{eCA}$ and control mice were subjected to PHx. Liver/bodyweight ratio was determined on days 2, 4, 6, and 8 post-PHx. (C,D) Liver samples were collected on days 2, 4, and 8 post-PHx, sectioned, and analyzed with anti-Ki67 IHC (C). The number of Ki67$^{+}$ cells was quantitatively compared (D). (E) Liver sections on PHx day 4 were analyzed by anti-Lyve-1 IF and SEM. Lyve-1$^{+}$ pixels and LSEC fenestrae were compared. Bars = means ± SD, n = 6; $^{*}P < 0.05$; $^{**}P < 0.01$; $^{***}P < 0.001$.

PHx, as shown by lowered liver weight/body weight ratio at each regeneration time point as compared to the control (Fig. 6B). Anti-Ki67 IHC showed that Notch activation in ECs significantly reduced hepatocyte proliferation in the process of PHx-induced LR (Fig. 6C,D). In addition, incomplete LSEC regeneration (Fig. 6E) and sustained capillarization (Fig. 6E) were observed in NIC$^{eCA}$ mice on day 4 post-PHx. Therefore, EC-specific Notch activation hampered LR post-PHx.

## LSECs WITH Notch ACTIVATION FAILED TO SUPPORT HEPATOCYTE PROLIFERATION DUE TO ATTENUATED Wnt LIGANDS AND HGF PRODUCTION

Comparison of gene expression profiles of LSECs showed that several hepatocyte mitogens, including Wnt2a, Wnt9b, and HGF, were down-regulated remarkably in NIC$^{eCA}$ LSECs (Fig. 7A). qRT-PCR confirmed down-regulation of HGF, Wnt2a, and Wnt9b in LSECs from NIC$^{eCA}$ mice (Fig. 7B). Furthermore, ELISA and western blotting also indicated that Notch activation down-regulated HGF and Wnt2a in LSECs at the protein level (Fig. 7C). These data suggested that EC-specific Notch activation impaired hepatocyte proliferation, likely through down-regulating paracrine Wnt ligands and HGF in LSECs.

Next, we cultured primary hepatocytes with CM from control or NIC$^{eCA}$ LSECs and examined hepatocyte proliferation. The result showed that CM from wild-type LSECs (Ctrl-CM) promoted hepatocyte proliferation, but CM from NIC$^{eCA}$ LSECs exhibited significantly reduced ability to stimulate hepatocyte proliferation as detected by anti-Ki67 IF (Fig. 7D,E). Of note, addition of HGF significantly restored the ability

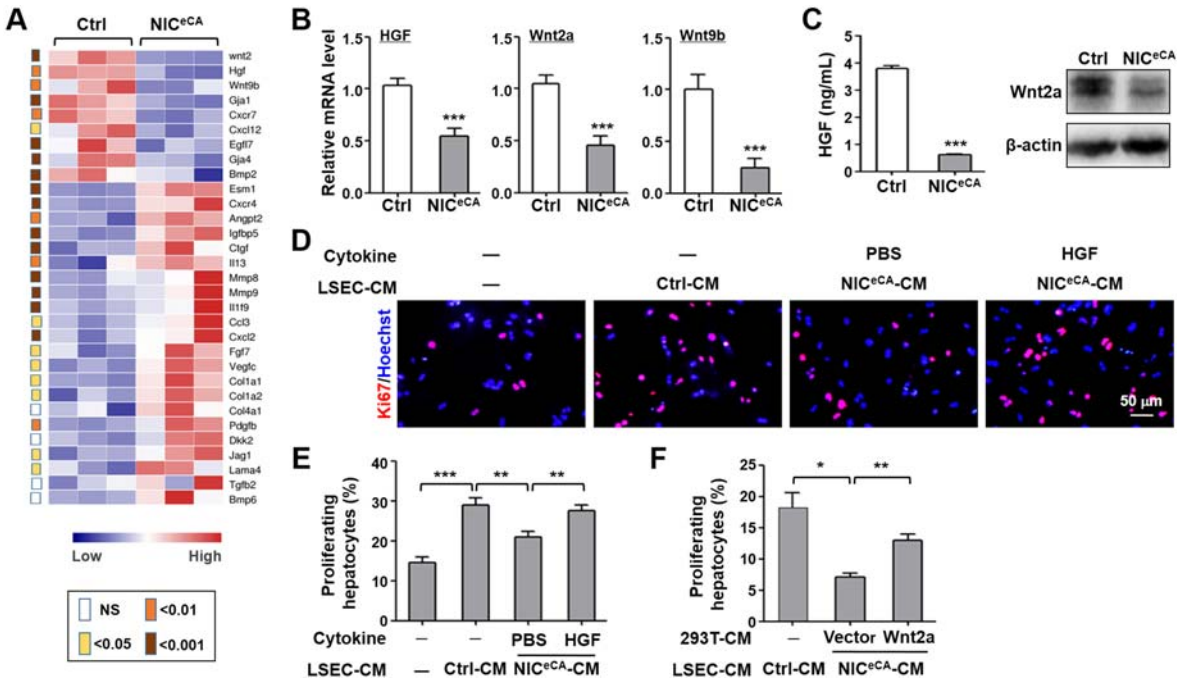


**FIG. 7.** Endothelial Notch activation attenuated hepatocyte proliferation by reducing Wnt ligands and HGF production. (A) Comparison of angiocrine-associated gene expression in LSECs from NIC$^{eCA}$ and control mice with a heatmap. The *P* value of each comparison was indicated with colors. (B) LSECs were isolated from the NIC$^{eCA}$ and control mice, and expression of HGF, Wnt2a, and Wnt9b was determined using qRT-PCR. (C) LSECs were isolated from NIC$^{eCA}$ and control mice and cultured *in vitro* for 48 hours. HGF in culture supernatants and Wnt2a in cell lysates were determined by ELISA and western blotting, respectively. (D,E) Normal hepatocytes were cultured with CM derived from LSECs of NIC$^{eCA}$ and control mice. PBS or recombinant murine HGF was added as indicated. Hepatocyte proliferation was determined with anti-Ki67 IF 48 hours later (D) and quantitatively compared (E). (F) Hepatocytes from normal mice were cultured with CM derived from LSECs of NIC$^{eCA}$ and control mice. Culture supernatants from *HEK293T* cells transiently transfected with pcDNA3.1 or pcDNA-Wnt2a were added (Supporting Fig. S4). Hepatocyte proliferation was determined with anti-Ki67 IF 48 hours later and quantitatively compared. Bars = means ± SD, n = 6; $^{*}P < 0.05$; $^{**}P < 0.01$; $^{***}P < 0.001$.

of NIC$^{eCA}$ LSECs to stimulate hepatocyte proliferation (Fig. 7D,E). Similarly, Wnt2a, which was derived from transfected *HEK293T* cells (Supporting Fig. S5), also partially rescued hepatocyte proliferation in culture with CM from NIC$^{eCA}$ LSECs (Fig. 7F). These results indicated that activation of Notch signaling in LSECs impaired hepatocyte proliferation, likely by down-regulating HGF and Wnt ligands.

## ENDOTHELIAL Notch ACTIVATION PERTURBED LSEC ANGIOCRINE FUNCTION THROUGH HETEROGENEOUS MECHANISMS

Next, we injected NIC$^{eCA}$ and control mice with the sGC activator, YC-1. The result showed that YC-1 rescued the morphological change of sinusoids in NIC$^{eCA}$ mice, as shown by H&E staining (Fig. 8A). Furthermore, YC-1 reversed decreased hepatocyte proliferation (Fig. 8A,B) and increased hepatocyte apoptosis (Fig. 8A,C), as well as increased hepatocyte damage in mice with endothelial Notch activation (Fig. 8D). Moreover, we examined the mRNA level of HGF, Wnt2a, and Wnt9b in isolated LSECs after YC-1 administration. The result showed that expression of Wnt2a and Wnt9b was up-regulated remarkably by YC-1 (Fig. 8E). However, expression of HGF was not rescued, but even further down-regulated in LSECs from NIC$^{eCA}$ mice after YC-1 administration (Fig. 8E). These data indicated that Notch activation regulated angiocrine function in LSECs by heterogeneous mechanisms: down-regulating Wnt2a and Wnt9b through repressing eNOS-sGC, and down-regulating HGF through other undefined signaling.

# Discussion

Inducible disruption of Notch1 or RBP-J using Mx-Cre resulted in abnormal sinusoidal remodeling, intussusceptive angiogenesis, and hepatic angiosarcomas.[29,30] To discriminate roles of Notch signaling in hepatocytes and LSECs, Cuervo et al. specifically disrupted RBP-J or Notch1 in LSECs, which resulted in altered sinusoidal structure and disturbed microcirculation.[31] It was observed that loss of function of Notch signaling leads to LSEC capillarization.[30] However, because LSECs are vulnerable to environmental insults such as shear stress,[5-9] the capillarization phenotype of LSECs in these loss-of-function models could be a consequence of tortuous sinusoids.[29-31] In the current study, we utilized a gain-of-function model of Notch signaling. Our gene expression profiling and morphological and LSEC functional data have indicated that endothelial Notch activation results in LSEC dedifferentiation. In the presence of $CCl_4$-induced liver

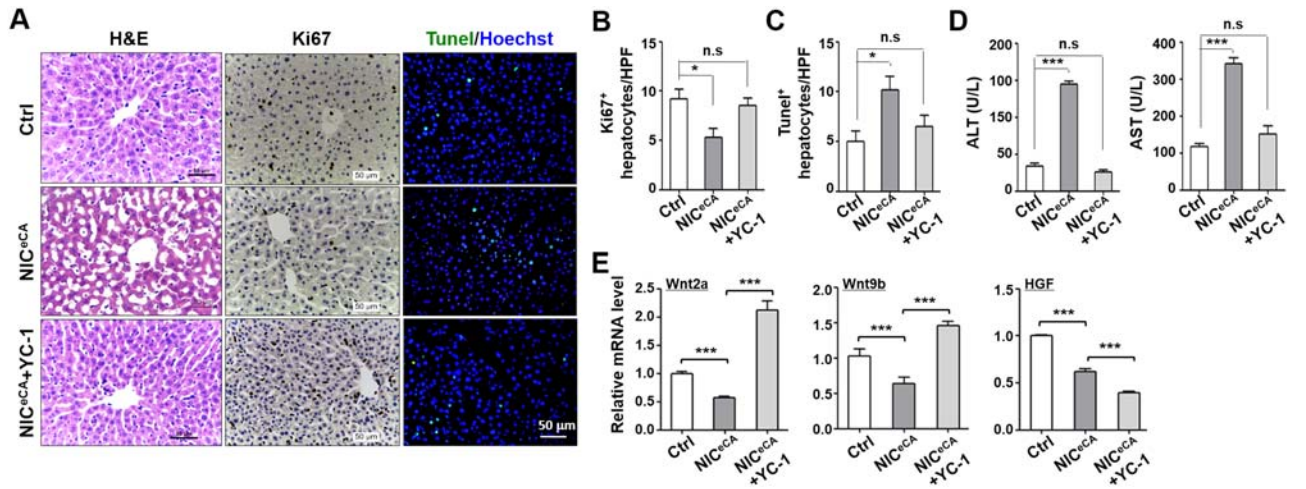


**FIG. 8.** sGC activator rescued hepatocyte proliferation as well as Wnt2a and Wnt9b expression attenuated by Notch activation. (A) NIC$^{eCA}$ and control mice were injected with YC-1 (Fig. 1A). Liver sections were stained by H&E, anti-Ki67 IHC, and TUNEL. (B,C) Numbers of Ki67$^+$ (B) and TUNEL$^+$ (C) hepatocytes were quantitatively compared. (D) Serum level of ALT and AST in the mice in (A) was determined. (E) LSECs were isolated and expression of Wnt2a, Wnt9b, and HGF was determined using qRT-PCR. Bars = means ± SD, n = 6; $^*P < 0.05$; $^{**}P < 0.01$; $^{***}P < 0.001$. Abbreviation: n.s, not significant.

damage, LSEC dedifferentiation promotes liver fibrogenesis, as demonstrated by many studies, likely through increased HSC activation attributed to up-regulation of TGF-$\beta$ and PDGF$\beta$.[10-13]

Notch activation-induced LSEC dedifferentiation could be attributed to attenuated eNOS-sGC signaling, which has been proven to maintain the differentiation of LSECs.[2,12,13] Indeed, in our study, an sGC activator efficiently rescued LSEC dedifferentiation induced by Notch activation. In NIC$^{eCA}$ mice, expression of eNOS was down-regulated at both mRNA and protein level. Moreover, activation of Notch signaling down-regulated VEGFR2 in LSECs. VEGFR2 is a receptor tyrosine kinase that can activate protein kinase B (Akt) that phosphorylates eNOS to maintain the differentiation of LSECs.[36] Therefore, Notch activation could skew down eNOS-sGC signaling through two mechanisms, in LSECs: directly down-regulating eNOS expression and reducing eNOS phosphorylation by down-regulating its upstream kinases, VEGFR2. This is quite different from the situation in continuous ECs. In cancer vasculature, inhibition of Notch signaling resulted in the down-regulation of eNOS.[37] Furthermore, it has been reported that Notch signaling up-regulates certain subunits of sGC in continuous ECs.[38,39] This inconsistency could be attributed to epigenetic difference between LSECs and continuous ECs, which show different gene expression profiles.[4] The mechanism for Notch activation-mediated eNOS down-regulation in LSECs is currently unknown. Bioinformatic analysis of the molecular interaction network suggests that Notch/RBP-J signaling might regulate eNOS through Hes1 or Hey1 (Supporting Fig. S6A).[27] In embryonic stem cells, chromatin immunoprecipitation sequence has shown that Hey1 binds to the eNOS promoter (Supporting Fig. S6B). More experiments are required to validate mechanisms for Notch activation-mediated down-regulation of eNOS in LSECs.

In addition to dedifferentiation, activation of Notch signaling modified the angiocrine spectrum of LSECs remarkably. Of note, several hepatocyte mitogens, including HGF, Wnt2a, and Wnt9b, were down-regulated significantly in LSECs upon Notch activation. Our *in vitro* culture assay has indicated that normal LSEC-derived conditional medium promotes hepatocyte proliferation, and this ability is abrogated by endothelial Notch activation. Addition of exogenous HGF or Wnt2 can rescue the effect of Notch activation, suggesting that Notch activation in LSECs damages hepatocyte proliferation by reducing the expression of HGF and Wnt ligands. This could be the reason of reduced hepatocyte proliferation of NIC$^{eCA}$ mice under both steady state and regeneration. In addition, Notch activation also up-regulates Angpt2, an EC-derived decoy ligand of Tie2, and competes with pericytes-derived Angpt1 to stimulate Tie2 receptor tyrosine kinase of ECs.[40] Aberrant expression of Angpt2 in LSECs with forced Notch activation might further damage LR by modulating hepatocyte proliferation and angiogenesis in phase I and phase II regeneration, respectively.[25]

Notch signaling might regulate the expression of different angiocrine factors with different mechanisms. Our data of profiling, qRT-PCR, and ELISA/western blotting indicated that HGF and Wnt levels were reduced in NIC$^{eCA}$ LSECs, accompanied with reduced hepatocyte proliferation. Although both HGF and Wnt rescued compromised pro-proliferation ability of NIC-LSECs *in vitro*, YC-1 rescued hepatocyte proliferation and Wnt expression, but not HGF expression *in vivo*, favoring a more important role of Wnt ligands. Therefore, the down-regulation of Wnt ligands (specifically Wnt2a and Wnt9b in our study) in LSECs with Notch activation is dependent on eNOS-sGC, and therefore associated with LSEC capillarization. On the other hand, Notch activation represses HGF expression in LSECs, most likely through other way(s) than eNOS-sGC. The mechanism of this disparity is unclear. Recently reports have suggested that bone marrow (BM)-derived LSEC progenitor cells (BM-SPCs) are dominant producers of HGF after liver injury. It is possible that Notch signaling regulates quiescent LSECs and BM-SPCs in different ways, leading to differential expression and regulation of Wnt and HGF.[41,42] More studies are needed to clarify how Notch signaling differentially regulates Wnt2a/9b and HGF.

In summary, hepatocytes undergo cell division to maintain homeostasis that is continuously challenged by endogenous and environmental stress signals.[19] Under steady state, hepatocytes secrete VEGF that, together with shear stress signal, maintains the differentiated state of LSECs through VEGFR2/Akt/eNOS.[5-8] Highly differentiated LSECs produce nitric oxide catalyzed by eNOS to guarantee low tension and maximum permeability of liver microcirculation, and repress HSC activation.[12,13,43] Quiescent LSECs also secrete Wnt2a/9b, which is downstream to eNOS-sGC signaling as demonstrated in the current study, to support hepatocyte proliferation.[18-21] Our data have shown that Notch, which responds to

various environmental stimuli such as VEGF and inflammation,[44,45] serves as a negative regulator of this circuit: Notch activation down-regulates eNOS-sGC signaling, leading to increased LSEC dedifferentiation, increased HSC activation and fibrosis, and reduced expression of Wnt2a/9b. Notch activation also represses the expression of HGF by LSECs and/or BM-SPCs through mechanisms other than eNOS-sGC (Supporting Fig. S7). During LR, Notch signaling was down-regulated through days 2 and 4 post-PHx to allow hepatocyte proliferation and vascular regeneration.

*Acknowledgments:* We thank Li H.L. and Adams R.H. for ROSA-STOP$^{floxed}$-NIC mice and CDH5-CreERT mice, respectively. This study was performed in the Graduates Innovation Center of Fourth Military Medical University.

## REFERENCES

1) Bataller R, Brenner DA. Liver fibrosis. J Clin Invest 2005;115:209-218.
2) **Poisson J**, **Lemoinne S**, Boulanger C, Durand F, Moreau R, Valla D, Rautou PE. Liver sinusoidal endothelial cells: physiology and role in liver diseases. J Hepatol 2017;66:212-227.
3) Nolan DJ, Ginsberg M, Israely E, Palikuqi B, Poulos MG, James D, et al. Molecular signatures of tissue-specific microvascular endothelial cell heterogeneity in organ maintenance and regeneration. Dev Cell 2013;26:204-219.
4) **Géraud C**, **Koch PS**, **Zierow J**, Klapproth K, Busch K, Olsavszky V, et al. GATA4-dependent organ-specific endothelial differentiation control liver development and embryonic hematopoiesis. J Clin Invest 2017;127:1099-1114.
5) DeLeve LD, Wang X, Hu L, McCuskey MK, McCuskey RS. Rat liver sinusoidal endothelial cell phenotype is maintained by paracrine and autocrine regulation. Am J Physiol Gastrointest Liver Physiol 2004;287:G757-G763.
6) Yokomori H, Oda M, Yoshimura K, Nagai T, Ogi M, Nomura M, Ishii H. Vascular endothelial growth factor increases fenestral permeability in hepatic sinusoidal endothelial cells. Liver Int 2003;23:467-475.
7) Shah V, Haddad FG, Garcia-Cardena G, Frangos JA, Mennone A, Groszmann RJ, Sessa WC. Liver sinusoidal endothelial cells are responsible for nitric oxide modulation of resistance in the hepatic sinusoids. J Clin Invest 1997;100:2923-2930.
8) Parmar KM, Larman HB, Dai G, Zhang Y, Wang ET, Moorthy SN, et al. Integration of flow-dependent endothelial phenotypes by Kruppel-like factor. J Clin Invest 2006;116:49-58.
9) Greuter T, Shah VH. Hepatic sinusoids in liver injury, inflammation, and fibrosis: new pathophysiological insights. J Gastroenterol 2016;51:511-519.
10) DeLeve LD. Liver sinusoidal endothelial cells in hepatic fibrosis. Hepatology 2015;61:1740-1746.
11) Xu B, Broome U, Uzunel M, Nava S, Ge X, Kumagai-Braesch M, et al. Capillarization of hepatic sinusoid by liver endothelial cell-reactive autoantibodies in patients with cirrhosis and chronic hepatitis. Am J Pathol 2003;163:1275-1289.
12) DeLeve LD, Wang X, Guo Y. Sinusoidal endothelial cells prevent rat stellate cell activation and promote reversion to quiescence. Hepatology 2008;48:920-930.
13) Xie G, Wang X, Wang L, Wang L, Atkinson RD, Kanel GC, et al. Role of differentiation of liver sinusoidal endothelial cells in progression and regression of hepatic fibrosis in rats. Gastroenterology 2012;142:918-927.
14) Rafii S, Butler JM, Ding BS. Angiocrine functions of organ-specific endothelial cells. Nature 2016;529:316-325.
15) Kostallari E, Shah VH. Angiocrine signaling in the hepatic sinusoids in health and disease. Am J Physiol Gastrointest Liver Physiol 2016;311:G246-G251.
16) DeLeve LD. Liver sinusoidal endothelial cells and liver regeneration. J Clin Invest 2013;123:1861-1866.
17) Marrone G, Shah VH, Gracia-Sancho J. Sinusoidal communication in liver fibrosis and regeneration. J Hepatol 2016;65:608-617.
18) Klein D, Demory A, Peyre F, Kroll J, Augustin HG, Helfrich W, et al. Wnt2 acts as a cell type–specific, autocrine growth factor in rat hepatic sinusoidal endothelial cells cross-stimulating the VEGF pathway. Hepatology 2008;47:1018-1031.
19) Ding BS, Nolan DJ, Butler JM, James D, Babazadeh AO, Rosenwaks Z, et al. Inductive angiocrine signals from sinusoidal endothelium are required for liver regeneration. Nature 2010;468:310-315.
20) Wang B, Zhao L, Fish M, Logan CY, Nusse R. Self-renewing diploid Axin2+ cells fuel homeostatic renewal of the liver. Nature 2015;524:180-185.
21) Rocha AS, Vidal V, Mertz M, Kendall TJ, Charlet A, Okamoto H, Schedl A. The angiocrine factor Rspondin3 is a key determinant of liver zonation. Cell Rep 2015;13:1757-1764.
22) LeCouter J, Moritz DR, Li B, Phillips GL, Liang XH, Gerber HP, et al. Angiogenesis-independent endothelial protection of liver: role of VEGFR-1. Science 2003;299:890-893.
23) Greene AK, Wiener S, Puder M, Yoshida A, Shi B, Perez-Atayde AR, et al. Endothelial-directed hepatic regeneration after partial hepatectomy. Ann Surg 2003;237:530-535.
24) Manavski Y, Abel T, Hu J, Kleinlutzum D, Buchholz CJ, Belz C, et al. Endothelial transcription factor KLF2 negatively regulates liver regeneration via induction of activin A. Proc Natl Acad Sci U S A 2017;114:3993-3998.
25) **Hu J**, **Srivastava K**, Wieland M, Runge A, Mogler C, Besemfelder E, et al. Endothelial cell-derived angiopoietin-2 controls liver regeneration as a spatiotemporal rheostat. Science 2014;343:416-419.
26) **Ding BS**, **Cao Z**, Lis R, Nolan DJ, Guo P, Simons M, et al. Divergent angiocrine signals from vascular niche balance liver regeneration and fibrosis. Nature 2014;505:97-102.
27) Gridley T. Notch signaling in vascular development and physiology. Development 2007;134:2709-2718.
28) Rostama B, Peterson SM, Vary CP, Liaw L. Notch signal integration in the vasculature during remodeling. Vasc Pharmacol 2014;63:97-104.
29) **Wang L**, **Wang CM**, **Hou LH**, Dou GR, Wang YC, Hu XB, et al. Disruption of the transcription factor recombination signal-binding protein-Jkappa (RBP-J) leads to veno-occlusive disease and interfered liver regeneration in mice. Hepatology 2009;49:268-277.

30) **Dill MT**, **Rothweiler S**, Djonov V, Hlushchuk R, Tornillo L, Terracciano L, et al. Disruption of Notch1 induces vascular remodeling, intussusceptive angiogenesis, and angiosarcomas in livers of mice. Gastroenterology 2012;142:967-977.
31) **Cuervo H**, **Nielsen CM**, Simonetto DA, Ferrell L, Shah VH, Wang RA. Endothelial notch signaling is essential to prevent hepatic vascular malformations in mice. HEPATOLOGY 2016;64: 1302-1316.
32) **Wang Y**, **Nakayama M**, **Pitulescu ME**, **Schmidt TS**, Bochenek ML, Sakakibara A, et al. Ephrin-B2 controls VEGF-induced angiogenesis and lymphangiogenesis. Nature 2010;465:483-486.
33) Monvoisin A, Alva JA, Hofmann JJ, Zovein AC, Lane TF, Iruela-Arispe ML. VE-cadherin-CreERT2 transgenic mouse: a model for inducible recombination in the endothelium. Dev Dyn 2006;235:3413-3422.
34) **Tian DM**, **Liang L**, **Zhao XC**, Zheng MH, Cao XL, Qin HY, et al. Endothelium-targeted Delta-like 1 promotes hematopoietic stem cell expansion ex vivo and engraftment in hematopoietic tissues in vivo. Stem Cell Res 2013;11:693-706.
35) Regina C, Panatta E, Candi E, Melino G, Amelio I, Balistreri CR, et al. Vascular ageing and endothelial cell senescence: molecular mechanisms of physiology and diseases. Mech Ageing Dev 2016;159:14-21.
36) Zhao Y, Vanhoutte PM, Leung SW. Vascular nitric oxide: Beyond eNOS. J Pharmacol Sci 2015;129:83-94.
37) Patenaude A, Fuller M, Chang L, Wong F, Paliouras G, Shaw R, et al. Endothelial-specific Notch blockade inhibits vascular function and tumor growth through an eNOS-dependent mechanism. Cancer Res 2014;74:2402-2411.
38) Chang AC, Fu Y, Garside VC, Niessen K, Chang L, Fuller M, et al. Notch initiates the endothelial-to-mesenchymal transition in the atrioventricular canal through autocrine activation of soluble guanylyl cyclase. Dev Cell 2011;21:288-300.
39) El-Sehemy A, Chang AC, Azad AK, Gupta N, Xu Z, Steed H, et al. Notch activation augments nitric oxide/soluble guanylyl cyclase signaling in immortalized ovarian surface epithelial cells and ovarian cancer cells. Cell Signal 2013;25:2780-2787.
40) Ribatti D, Nico B, Crivellato R. The role of pericytes in angiogenesis. Int J Dev Biol 2011;55:261-268.
41) Wang L, Wang X, Xie G, Wang L, Hill CK, DeLeve LD. Liver sinusoidal endothelial cell progenitor cells promote liver regeneration in rats. J Clin Invest 2012;122:1567-1573.
42) Wang L, Wang X, Wang L, Chiu JD, van de Ven G, Gaarde WA, Deleve LD. Hepatic vascular endothelial growth factor regulates recruitment of rat liver sinusoidal endothelial cell progenitor cells. Gastroenterology 2012;143:1555-1563.
43) **Marrone G**, **Russo L**, Rosado E, Hide D, Garcia-Cardena G, Garcia-Pagan JC, et al. The transcription factor KLF2 mediates hepatic endothelial protection and paracrine endothelial–stellate cell deactivation induced by statins. J Hepatol 2013;58:98-103.
44) Benedito R, Hellstrom M. Notch as a hub for signaling in angiogenesis. Exp Cell Res 2013;319:1281-1288.
45) Borggrefe T, Lauth M, Zwijsen A, Huylebroeck D, Oswald F, Giaimo BD. The Notch intracellular domain integrates signals from Wnt, Hedgehog, TGF$\beta$/BMP and hypoxia pathways. Biochim Biophys Acta 2016;1863:303-313.

Author names in bold designate shared co-first authorship.

# Supporting Information

Additional Supporting Information may be found at onlinelibrary.wiley.com/doi/10.1002/hep.29834/suppinfo.